Applied Surface Science 567 (2021) 150848

Contents lists available at ScienceDirect

Applied Surface Science

journal homepage: www.elsevier.com/locate/apsusc

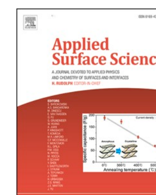

Full Length Article

Stabilization of unstable and metastable InP native oxide thin films by interface effects

M.P.J. Punkkinen *, A. Lahti, J. Huhtala, J.-P. Lehtiö, Z.J. Rad, M. Kuzmin [1], P. Laukkanen, K. Kokko

Department of Physics and Astronomy, University of Turku, Turku FI-20014, Finland

ARTICLE INFO

Keywords:
Interface energy
III-V semiconductor
Oxide
Coherence
Band gap
DFT

ABSTRACT

III-V semiconductor - oxide interfaces have attracted huge interest due to their substantial potential in electronic applications. However, due to the extreme complexity of the modeling of the interfaces, there are only few *ab initio* studies of these interfaces.

Several model interfaces of native $InPO_4$ oxides are designed in this study. It is shown that energies of the (quasi-)coherent interfaces are much smaller than energies of the incoherent interfaces. Furthermore, it is pointed out that the interface energy can stabilize oxide structures not found in bulk form. Relatively small strain energy and configurational match imply a small interface energy.

It is estimated that the gap state density of the In-terminated quasi-coherent interfaces is small or zero. However, partial oxidation of the substrate P atoms, which can be induced, *e.g.*, by non-stoichiometry of the oxide, causes distinct gap states. This is a mechanism to explain Fermi level pinning of the III-V – oxide interfaces. Non-stoichiometric compositions are also investigated. Experimental results on InP native oxide growth are discussed. The models can be used to study various properties of the interfaces and more complex models including, *e.g.*, dislocations or non-planar surfaces can be based on the models.

1. Introduction

There is a significant gap between experimental results and modeling of oxide interfaces due to the extreme complexity of these interfaces [1]. This is particularly true of III-V semiconductor interfaces. Lattice, configurational and electronic mismatches are serious obstacles for modeling of these interfaces. The electronic mismatch is expressed in terms of the electron counting rule (ECR), which is supposed to act during oxide growth or deposition and drive the creation of interface defects [2,3]. In addition, the III-V semiconductors can form a rich variety of compositionally different oxides.

The native oxide interfaces of the III-V semiconductors have been investigated intensively for a very long time due to their immense potential in semiconductor electronics [4,5]. However, the native oxide interfaces have generally many interfacial defects, which cause electrical losses in current applications such as light emitting diodes, infrared detectors and high electron mobility transistors (HEMT). It is difficult to avoid the formation of the native oxides in these devices. The native oxides have also hindered the development of the III-V metal-–oxide-semiconductor transistors. Although the current flows at the heteroepitaxial III-V interface in the state-of-the-art HEMT devices, the increased performance criteria require nowadays understanding and controlling the HEMT gate area as well, which readily includes the III-V native oxides. In contrary to general consensus, some studies reveal that specific native oxide thin films increase the quality of the III-V semiconductor-oxide interfaces [6–9].

Native oxide interfaces of indium phosphide (InP) are investigated in this study. We focus especially on the $InPO_4$/InP interface. The phase separation of the bulk $InPO_4$ into bulk indium oxide and phosphorus oxide ($2{\bullet}InPO_4 \rightarrow In_2O_3 + P_2O_5$) is thermodynamically inhibited [10]. This can be unambiguously estimated, because In_2O_3 and P_2O_5 oxides are favored (arsenic is oxidized into As_2O_3 instead of As_2O_5). Furthermore, an $InPO_4$ oxide film can be formed in principle by oxidizing the InP without In or P outdiffusion. To the best of our knowledge there are only few (interface) models of the III-V native oxides [11] and the atomic interface structures are unknown. Some models have been

* Corresponding author.
E-mail address: marpunk@utu.fi (M.P.J. Punkkinen).
[1] address: Ioffe Physical-Technical Institute, Russian Academy of Sciences, St. Petersburg 194021, Russian Federation

https://doi.org/10.1016/j.apsusc.2021.150848
Received 17 March 2021; Received in revised form 30 June 2021; Accepted 1 August 2021
Available online 5 August 2021
0169-4332/© 2021 The Author(s). Published by Elsevier B.V. This is an open access article under the CC BY license (http://creativecommons.org/licenses/by/4.0/).

introduced previously for the HfO_2/III-V [12–17] and Al_2O_3/III-V and Gd_2O_3/III-V [13,14,18,19,20] interfaces having non-native oxides. Adsorption of O atoms and molecules on the III-V substrates has also been investigated [7,21–23].

Generally bulk oxide structures matching the III-V substrate in terms of lattice match (lattice parameters), atomic configuration match and electronic match (ECR) do not exist. Therefore, we construct interface structures using unstable bulk oxide structures. These configurationally and electronically matched oxides have smaller strain energies, induced by coherent growth, than stable and metastable oxides found in literature generally have. The interface models constructed using unstable oxides are coherent in the initial stage before relaxations. A coherent interface model is shown in Fig. 1(a). Other interface model type is an incoherent one (lattice and atomic configuration mismatch), which is constructed using the $InPO_4$ oxide, which corresponds to the ground state at ambient pressures [Fig. 1(b)]. If the lattice mismatch is reasonable, a coherent interface can be transformed into a semi-coherent one by misfit dislocations.

Interface energies are determined in this study, which in itself, is a quite complicated and cumbersome task for the interface systems considered. It is studied, whether the interface can stabilize oxide structures obtained from the initially coherent interfaces. This also suggests, whether the interfaces have energies low enough to be considered satisfactory to model real interfaces and good starting points to design more complicated structures which are beyond the *ab initio* calculations. The ECR is satisfied in the initially coherent models by a designed compositionally relevant low energy surface structure. The interfaces do not include substitutional atoms leading to unmanufacturable interfaces [2] or vacancies leading to increasing of the interface energy. The initially coherent model is relatively simple and small and it is not specific to a certain interface area. These are important beneficial features of the model.

Further insight into interface defects and the formation of the experimentally found peculiar ordered or crystalline oxide film [7] is also obtained by the models and results presented. Experimentally, the main source of information, photoelectron spectroscopy, gives only indirect information about the structures. Interpretation is commonly based on the “fingerprints” of the bulk oxides, *i.e.*, the core-level binding energies obtained from photoelectron spectra measured for separate bulk oxides. This ignores interface effects, including band offsets at the interfaces. These interface effects may be important especially, if core-level shifts energetically close to each other are analyzed, which is often the case. Furthermore, growth temperature and cleaning procedures affect oxide film composition and structure. The structural models and results given in this study embody a step towards modeling the photoelectron spectra detected in experiments under varying conditions more accurately.

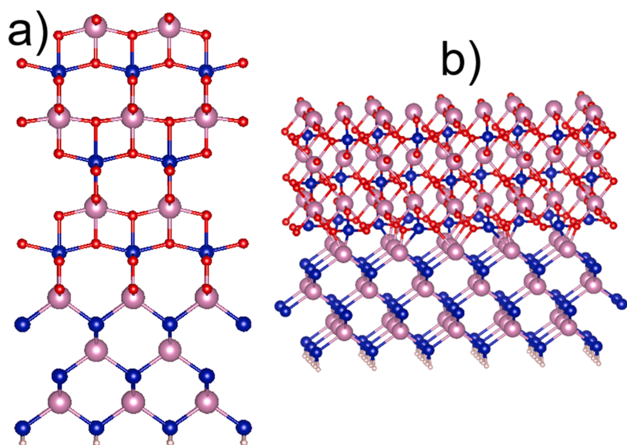

Fig. 1. At the coherent interface there is an atomic layer which semiconductor and oxide film “share” due to perfect atomic configuration match (a). An incoherent interface, in which both atomic configurations and lattice constants in semiconductor and oxide deviate significantly (b). The atomic structures shown are used in this study. The In, P and O atoms are shown by (large) violet, (intermediate size) blue and (small) red spheres, respectively.

2. Computational methods

Calculations were performed using an *ab initio* density functional theory (DFT) total energy method within the Perdew-Burke-Ernzerhof (PBE) generalized gradient approximation (GGA) [24]. The approach is based on the plane wave basis and projector augmented wave method [25,26] (Vienna *ab initio* simulation package, VASP) [27–30]. Optimization of the atomic structures was performed using conjugate gradient minimization of the total energy with respect to atomic coordinates. Atoms were relaxed until remaining forces were less than 20 meV/Å. Plane wave cutoff energy was chosen to be 350 eV for the interface and surface calculations. It was found that this cutoff energy provides sufficient accuracy for slab calculations [17]. Bulk calculations were performed using a cutoff of 500 eV and similarly sized supercells to obtain accurate relative total energies. The In and P 3d electrons were treated as core electrons.

Surface and interface areas are expressed using the Wood’s notation. The InP (001) surface area within the Wood’s notation is expressed in terms of the primitive translation vector of the bulk zincblende structure, which is about 4.24 Å for the face-centred cubic InP within the PBE. The interface area in the initially coherent interfaces was (2×2) or $c(4 \times 4)$. The interface areas of the incoherent interfaces are given in subsection 3.1. The k point sampling was carried out by the Monkhorst-Pack scheme [31] using a $3 \times 3 \times 1$ mesh for a (2×2) InP interface area and a $2 \times 2 \times 1$ mesh for larger interface areas. The origin was shifted to the Γ point.

The interface systems were modeled using slab unit cells including vacuum. The width of the vacuum was at least 15 Å. The initially coherent interfaces were constructed using unstable $InPO_4$ bulk oxide structures [32]. The first model bulk oxide ($InPO_4$-a) is based on the tetragonal TiO_2-type (anatase) HfO_2 structure [33] (space group 141). Every second Hf atomic layer in the direction of the longest lattice parameter is substituted with either In or P atoms. The space group number of this structure is 119 and the Wyckoff positions 2a, 2d, 4e ($z = 0.047$) and 4f ($z = 0.203$) are occupied. The doubling of the unit cell in the [001] direction (along the c lattice parameter) decreases total energy as PO_4 tetrahedra can be oriented in different ways. The second model bulk oxide structure ($InPO_4$-b) is tetragonal and the space group number of the structure is 80. The square face of the tetragonal cell has an InP (2×2) area and the optimal c lattice parameter value is about 16.2 Å. The Wyckoff positions are shown in Table 1. The model bulk oxide structures are shown in Fig. 2. The oxide structures are relaxed quite significantly during structural optimization. Incoherent interfaces were modeled using $CrVO_4$-type orthorhombic oxide structure (space group 63) in which the $InPO_4$ oxide crystallizes at ambient conditions [34]. The lattice parameter values of $a = 5.38$ Å, $b = 8.17$ Å and $c = 6.94$ Å were obtained. Cutting planes of the oxide were (100) and (001). The InP semiconductor part of the interface was terminated by a (001) surface. [The (100), (010) and (001) InP surfaces are equivalent.]

An oxide part and a semiconductor part are joined to form an

Table 1
Wyckoff positions of an unstable tetragonal coherent oxide having the space group number 80, $InPO_4$-b.

	x	y	z
In (4a)			0.697
P (4a)			0.098
O1 (8a)	0.232	0.301	0.297
O2 (8a)	0.778	0.160	0.160

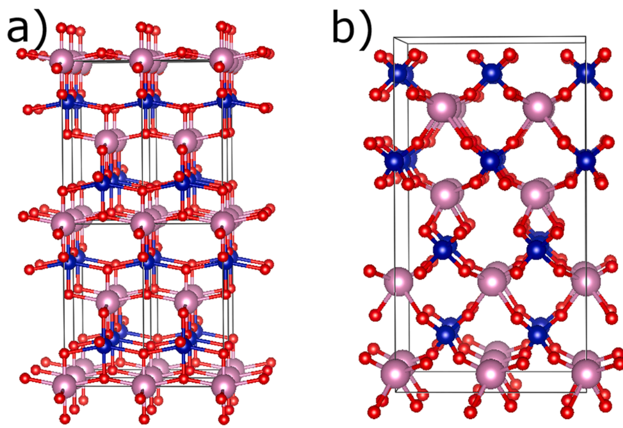

Fig. 2. Tetragonal $InPO_4$-a (a) and $InPO_4$-b (b) structures used as initial coherent structures. The bottom and top surfaces of the unit cells shown comprise a (2 × 2) InP area. The In, P and O atoms are shown by (large) violet, (intermediate size) blue and (small) red spheres, respectively.

interface system. Additional or excess O atoms, relative to the oxide part (stoichiometric composition), can be introduced in suitable positions at the interface. The semiconductor part of the unit cells consist of three layers of group III atoms and three layers of group V atoms. The bottom layer atoms of the semiconductor part are passivated by pseudo-hydrogen atoms. The positions of the In and P atoms closest to the pseudo-hydrogen layer are fixed to the ideal positions. The thickness of the oxide part was varied. The interfaces are characterized by the cutting planes of the oxide, because there is only one cutting plane of the InP. The (0 0 1) interfaces of the III-V compound semiconductors are widely used in device applications. The initially coherent or quasi-coherent oxide structures presented in this manuscript are best matched to the (0 0 1) atomic layers of the InP.

Relative stabilities of different initially coherent and incoherent oxide films are determined by calculating relative total energies using *ab initio* atomistic thermodynamics [35,36]. The stability of the oxide as well as the thickness of the oxide are important factors contributing to the total energy in addition to the interface and surface energies. Generally total energies of the initially coherent and incoherent interface systems can not be directly compared, because the number and types of atoms are not exactly the same in the compared systems.

The relative total energy $E_{\rm rel}$ is calculated for the most of the considered oxide films as follows

$$E_{rel} = aE_{\rm incoh} - \Delta N_{\rm InPO4}\mu_{\rm InPO4} - \Delta N_{\rm O,ex}\mu_{\rm O} - E_{\rm coh} \quad (1)$$

where $E_{\rm incoh}$ and $E_{\rm coh}$ are the total energies of the incoherent and initially coherent interface systems, respectively. The factor a ensures that the interface area and thus the number of substrate atoms as well as pseudo-hydrogen atoms are the same in the compared incoherent and initially coherent interface systems. The $\Delta N_{\rm InPO4}$ and $\Delta N_{\rm O,ex}$ denote differences in the numbers of the $InPO_4$ units and excess O atoms between the incoherent and initially coherent interface systems. The interfaces are generally oxygen-rich. Thus, there are in addition to the $InPO_4$ units some additional O atoms, which are called excess O atoms. The $\mu_{\rm InPO4}$ and $\mu_{\rm O}$ are the chemical potentials of the $InPO_4$ and O. The chemical potentials of the In_2O_3 and P_2O_5 are also needed for a few of the interfaces. The chemical potentials of the $InPO_4$, In_2O_3 and P_2O_5 are set equal to the corresponding bulk energies. The chemical potential of the O is a variable.

The bulk ground state $InPO_4$ total energy, needed to calculate surface and interface energies, was obtained using the incremental method [37], in which pure $InPO_4$ slabs with different thicknesses are used. This is a usual method to increase the accuracy of the surface and interface energies, because errors tend to be partially cancelled by using similar calculational parameters and settings for bulk and surfaces/interfaces.

The upper limit of the O chemical potential is obtained by the total energy of an O_2 molecule (total energy of an O_2 molecule divided by two). The lower limit is obtained by summing the upper limit and the formation energy of the bulk $InPO_4$ (negative) per O atom, which is obtained by using the InP bulk chemical potential. The chemical potential of the bulk InP is equal to the chemical potentials of bulk In [38] and P [39] plus the formation energy of the bulk InP (negative). The chemical potential of an O atom in the O_2 molecule is −4.92 eV within the PBE and the formation energy of the $InPO_4$ is −11.85 eV. The absolute value of the O chemical potential is about 5–6 eV under common experimental growth conditions [17].

Relative stabilities of different incoherent oxide films can be estimated by calculating interface energies, because the total energy of the oxide film is accurately the same in different incoherent oxide films. The absolute interface energies are calculated for the incoherent interfaces using the following equation:

$$\gamma_I A = E_{\rm incoh} - N_{\rm InP}\mu_{\rm InP} - N_{\rm InPO4}\mu_{\rm InPO4} - N_{\rm O,ex}\mu_{\rm O} - N_{\rm H^*}\mu_{\rm H^*} - \gamma_S A \quad (2)$$

where γ_I, γ_S and A denote the interface energy, surface energy of the oxide and interface/surface area, respectively. The H* denotes a pseudo-hydrogen atom. The chemical potential of the H* includes the contribution of the surface energy of the pseudo-hydrogenized surface. We have used two types of pseudo-hydrogen atoms ($Z = 0.75$ and $Z = 1.25$). The interface energy describes the stability of the interface layer(s), whereas the total energy reflects also the stability of the oxide film and is dependent on the film thickness.

The interface energies of the initially coherent interfaces could not be determined, because it turned out that surface energy could not be estimated for the corresponding oxide surface. There is probably no bulk volume in thin surface slabs. Quite large surface slabs (~40 Å thick) would be needed to get equal surfaces and different thicknesses for the incremental method, and it seems that relaxation from the unstable initial structures might not be as efficient as in the interface calculations. However, sums of the surface and interface energies of the incoherent and initially coherent interfaces were compared.

3. Results and discussion

3.1. Incoherent interface structures and energies

Interface energies of the incoherent interfaces are determined next. Key factors are atomic layer configurations, the lattice mismatch and the electronic (mis)match described by the ECR. In the [1 0 0] direction O layers and layers consisting of In, P and O atoms (In-P-O layers; composition $InPO_2$) alternate. In the [0 0 1] direction In-O (composition InO_2) and P-O layers (composition PO_2) alternate. The (1 0 0) and (0 0 1) atomic layers are shown in Fig. 3. In the [0 1 0] direction it is more difficult to determine separate atomic layers. The structure might be considered to consist of In-O and P-O layers of which the P-O layers are not smooth. Therefore, it is expected that the incoherent (0 1 0) interface energies are relatively large. Furthermore, the needed (0 1 0) interface area to obtain acceptable lattice mismatch is large [(5 × 5) InP (0 0 1) area]. The same reasoning applies to interfaces having larger Miller indices. The oxide surface becomes less planar as the Miller indices are increased, which generally means that fewer bonds across the interface are formed. Second, it is supposed that overlapping of the atoms in semiconductor and oxide layers is weaker, when the symmetry of the oxide layer decreases with increasing Miller indices. All bonds across the O-rich (0 0 1) interfaces are energetically most favorable In-O-P type bonds. Weaker bonds are formed across the interfaces, if high-index oxide layers are attached to the semiconductor. Therefore, the (1 0 0) and (0 0 1) interfaces are considered.

Relatively oxygen-rich interfaces are the most stable ones under typical experimental conditions [15–17]. The (1 0 0) interfaces were formed by attaching an oxygen-terminated oxide part (and not the In-P-O terminated oxide part) to the semiconductor substrate. The

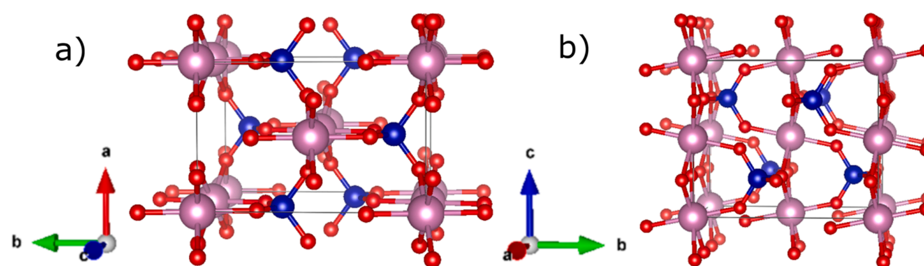

Fig. 3. Atomic layers of the ground state $InPO_4$ along the [1 0 0] (a) and [0 0 1] (b) directions. The P and O atoms form one layer (P-O layer), whereas In atoms and O atoms form another layer (In-O layer) along the [0 0 1] direction. The O and In atoms are not exactly within the same plane within the In-O layer. The In, P and O atoms are shown by violet, blue and red spheres, respectively.

semiconductor is either In-terminated or P-terminated. The In-terminated semiconductor was joined with a P-O layer and the P-terminated semiconductor was joined with an In-O layer at the (0 0 1) interfaces. The interfaces are characterized by the terminations of the semiconductor for clarity. A (1 × 3) $InPO_4$ (1 0 0) area was attached to a (2 × 5) InP (0 0 1) area with $InPO_4$ lattice mismatches of −3.9 % and −1.9 % along the $InPO_4$ y- and z-directions, respectively. The lattice mismatches are estimated using the calculated bulk lattice parameters. A (4 × 1) $InPO_4$ (0 0 1) area was attached to a (5 × 2) InP (0 0 1) area with $InPO_4$ lattice mismatches + 1.5 % and −3.9 % along the $InPO_4$ x- and y-directions, respectively. It was found that the strain energy is only about 7–9 meV per atom. The (1 0 0) and (0 0 1) interface areas are doubled along the shorter interface lattice parameter to satisfy the ECR [3,17]. There are about 400–550 atoms in the largest slab cells, which makes calculations very heavy and slow.

The surface energies were calculated for various (1 0 0) and (0 0 1) surfaces to find relatively stable oxide surfaces needed for the interface slab cells. Previous results for the $InPO_4$ surfaces were not found in literature. The surface In and P atoms lose O neighbors at the surface. The remaining O atoms (half of the bulk O layer) are bonded to the P atoms at the (1 × 1) $InPO_4$ (1 0 0) surface [see Fig. 3(a)]. There is only one type of oxide termination at the (1 0 0) surface. A (2 × 1) $InPO_4$ area is needed for the (0 0 1) surface due to the ECR. This is obtained either by introducing one O vacancy within an In-O layer at the In-terminated surface or adding one O atom on a P-O layer at the P-terminated surface [see Fig. 3(b)]. The In-terminated (2 × 1) $InPO_4$ (0 0 1) surface is strongly reconstructed to increase the coordination number of the "lone" O atoms (one-coordinated O atoms) at the surface. The (1 0 0) surface energy is 81.7 meV/Å^2. The surface energies of the In-O-terminated and P-O-terminated (0 0 1) surfaces are 77.0 meV/Å^2 and 72.4 meV/Å^2, respectively. It is noted that the (0 0 1) surface slabs are not stoichiometric. Therefore, incremental In_2O_3 (bixbyite) [40] and P_2O_5 [41] bulk energies are also used for the estimation of the surface energy.

It is remarkable that the periodicity of the O atoms is similar to the periodicity of the semiconductor atoms along the shorter interface lattice parameter. Each In or P atom at the interface layer of the semiconductor part is bonded initially at least to one O atom, if the positions of the atoms are chosen appropriately. Some initial positions of the atoms at the (1 0 0) and (0 0 1) interfaces are shown in Fig. 4. It was found, by varying the horizontal coordinates of the oxide part, that the lowest total energies are obtained by these initial positions.

A stoichiometric (1 × 3) $InPO_4$ (1 0 0) oxide part has a half-filled oxygen layer at the surfaces (six O atoms). The (1 × 3) $InPO_4$ (1 0 0) oxide part attached to the semiconductor substrate has a full oxygen layer at the interface (12 O atoms). Therefore, the oxide part lacks 12 electrons due to the extra O atoms relative to the corresponding stoichiometric surface slab. There are six excess O atoms. [Compare the O layer at the interface and the O layer at the surface in Fig. 3(c).] On the other hand, the (4 × 1) $InPO_4$ (0 0 1) oxide part either lacks four electrons (In-termination at the interface) or has four extra electrons (P-termination at the interface) relative to the corresponding ECR obeying stoichiometric oxide part due to the additional/excess (In-termination) or missing (P-termination) O atom per oxide (2 × 1) area. There are 10 In or P atoms within the semiconductor surface layer. The In and P atoms, which are less electronegative than an O atom, donate electrons. An In atom donates either 1.5 or 0.5 electrons and a P atom donates either 2.5 or 1.5 electrons to the oxide part depending on whether the atom forms a dimer bond with a neighboring In or P atom or not. If a P atom does not form a dimer bond, a fully occupied P dangling bond consuming two electrons may be formed. A dimer bond can be substituted by an O bridge. The ECR is satisfied by choosing a particular number of dimer (or bridge) and dangling bonds.

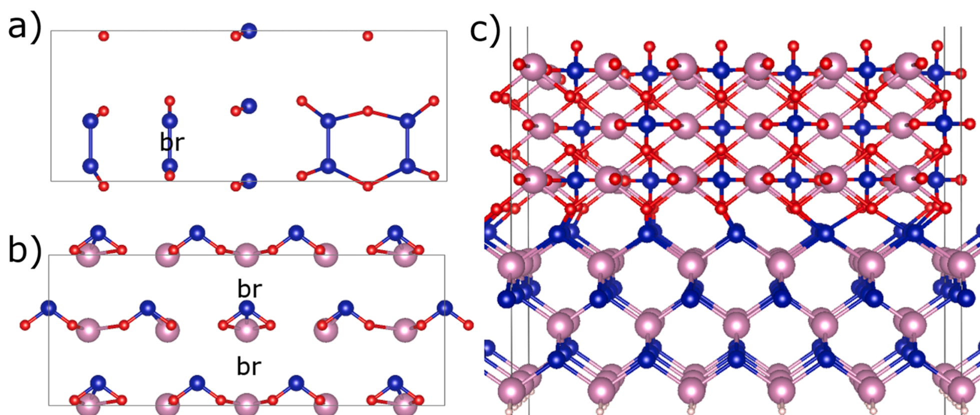

Fig. 4. Initial positions of the atoms closest to the incoherent interface at the P-terminated semiconductor (1 0 0) interface (a) and at the In-terminated semiconductor (0 0 1) interface (b). The atoms of the P-terminated (1 0 0) interface unit cell (c). The periodicity of the O atoms is similar to the periodicity of the semiconductor atoms along the shorter interface lattice parameter. Similar interface O atom positions are used for other terminations. The P atoms are dimerized at the (1 0 0) interface. One of the P dimers is broken (two P dangling bonds) to bind additional electrons. The interface areas have to be doubled and a particular number of dimer and dangling bonds chosen to obey the ECR. These interfaces do not include additional O atoms (relative to the non-stoichiometric oxide part), which can be inserted into the semiconductor bridge sites or vertical bridge sites across the interface. Some semiconductor (horizontal) bridge sites (br) are shown. The In, P, O and pseudo-hydrogen atoms are shown by violet, blue, red and grey spheres, respectively.

The (1 0 0) oxide part includes three In-P-O layers and three and half O layers (the half-filled O layer at the oxide surface), whereas the (0 0 1) oxide part includes two In-O layers and two P-O layers. The thicknesses of the oxide parts are very similar, about 5.2–5.4 Å. The In or P atoms initially at the semiconductor surface can form bridge bonds with additional O atoms. Therefore, the interfaces can be O-enriched. The border between the semiconductor and oxide parts has to be defined to enable energy comparisons between different interfaces. In the following, the O atoms are not allowed to penetrate into the In-P bonds within the semiconductor part.

The P-terminated interfaces can be more O-rich than the In-terminated interfaces, because P atoms have more electrons than the In atoms have in their outermost shell. The interface energies of the P-terminated (1 0 0) interface and the In-terminated (0 0 1) interface are the lowest ones. Selected interface energies are shown in the interface energy diagram in Fig. 5. If there are no available electrons for ionic bonds, the interface energy can even be increased with the additional O atoms. This was found to happen at the In-terminated (1 0 0) interface. The P-terminated interfaces do not show an energy gap. Substrate P atoms having both covalent and ionic bonds induce gap states. Furthermore, after relaxations some oxygen atoms form bonds also with the substrate In atoms below the substrate P atoms.

One can note that the interface energies can be negative, because cohesive energy is strongly increased by the additional O atoms. The maximum number of the excess O atoms per (1 × 1) interface area is 0.75 for both the In-terminated (1 0 0) and (0 0 1) interfaces. The corresponding values for the P-terminated (1 0 0) and (0 0 1) interfaces are 1.5 and 1.2, respectively. The interface energy decreases with the additional O atoms for a particular substrate termination and oxide cut as usual. However, the relative interface energies of the In-terminated and P-terminated (1 0 0) and (0 0 1) interfaces can not be explained accurately using the (maximum) number of the excess O atoms. Bond number and bond type are important factors. For example, there are more atoms, which form bonds with the substrate atoms, within the oxide P-O layer than within the oxide In-O layer at the (0 0 1) interfaces. This is due to the smoothness of the P-O layers in the $InPO_4$ oxide along the [0 0 1] direction. It is concluded that this is one factor stabilizing the In-terminated (0 0 1) interface relative to the P-terminated (0 0 1) interface. There are only In-O-P bonds, which are more stable than the In-O-In and P-O-P bonds, across the (0 0 1) interface plane stabilizing the (0 0 1) interfaces.

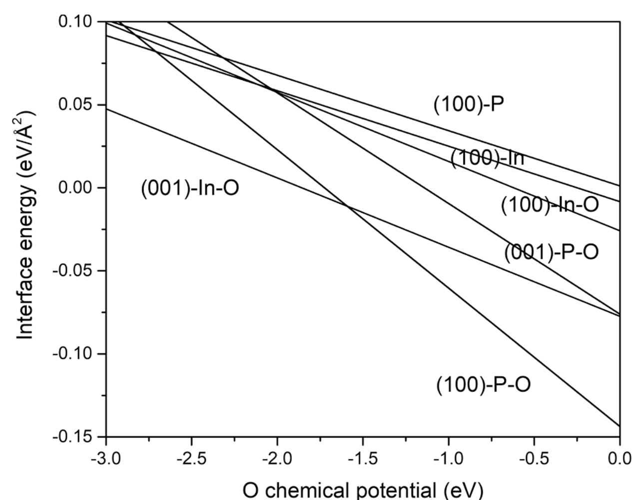

Fig. 5. The absolute interface energies of some selected incoherent interfaces. The O chemical potential is expressed relative to the upper limit of the O chemical potential. The (1 0 0)-In and (1 0 0)-P denote the In- and P-terminated (1 0 0) interfaces with no additional O atoms relative to the non-stoichiometric oxide part. The (1 0 0)-In-O and (0 0 1)-In-O denote the In-terminated (1 0 0) and (0 0 1) interfaces having maximum number of the excess O atoms defined by the ECR. The (1 0 0)-P-O and (0 0 1)-P-O denote the P-terminated interfaces having the maximum number of the excess O atoms not occupying the substrate In-P bonds. These P-terminated interfaces do not show an energy gap

The interface energy of the In-terminated (0 0 1) interface becomes similar to that of the P-terminated (1 0 0) interface with the largest O chemical potential, if 0.4 excess O atoms per (1 × 1) interface area are removed from the P-terminated (1 0 0) interface. The amount of the O atoms could be limited kinetically, *e.g.*, due to limited O diffusion. If the number of the removed excess O atoms is 0.2 at the P-terminated (1 0 0) interface, the interface energies become similar with the relative O chemical potential around −1 eV, which is reached under suitable growth conditions [17]. The constraint to rule out oxygen atoms penetrating into the substrate bonds is somewhat arbitrary, because oxygen atoms form other bonds with the substrate In atoms at the P-terminated (1 0 0) interface. It is important to note that the same number of excess O atoms at the P-terminated and In-terminated interfaces is reached for all P-terminated or In-terminated interfaces, if deeper substrate layers are occupied for partial interface areas. For example, the relative total energy of the In-terminated (0 0 1) interface system is lower than that of the P-terminated (1 0 0) interface system having the maximum number of excess O atoms, if interface edge energies induced by areas having different number of oxide layers are omitted. Here, it is energetically more favorable to use some excess O atoms to oxidize deeper layers than to further oxidize the interface. The same conclusion is obtained by comparing less O-rich In-terminated (0 0 1) and P-terminated (1 0 0) interfaces. Therefore, it may be physically relevant to compare energies of interfaces having the same amount of excess O atoms. One could think that it is always energetically more favorable to oxidize deeper layers, but this is not the case. The formation energy of the bulk $InPO_4$ obtained oxidizing bulk InP is about 7.88 eV per O atom. For example, the O enrichment of the In-terminated (0 0 1) and P-terminated (1 0 0) interfaces is energetically more favorable than the oxidation of the deeper layers until the number of excess O atoms per (1 × 1) area is about 0.5–0.6 and 1.1, respectively.

3.2. *Quasi-coherent interfaces and oxide film growth*

The initially coherent interfaces are formed using the oxide structures introduced in Section 2. However, the structure and total energy can be relaxed significantly by breaking the initial symmetry of the $InPO_4$-a and $InPO_4$-b structures. This can be done by non-symmetric displacements of the atoms in the initial structure. (It is usually enough to shift one atom.) The square face area of the tetragonal unit cell used is fixed to the substrate InP (2 × 2) area. A surface reconstruction similar to the ground state oxide (0 0 1) surface is used by introducing one O vacancy per InP (2 × 2) area. Typically the obtained total energies of the relaxed $InPO_4$-a and $InPO_4$-b are astonishingly close to each other. The incremental bulk energy of the relaxed $InPO_4$-a or $InPO_4$-b, “alpha” $InPO_4$, is taken from the interface calculations. The available incremental energies (the thickest films are almost 2 nm thick) are 100–125 meV per atom above the total energy of the ground state $InPO_4$. A structure obtained from a bulk calculation is shown in Fig. 6.

There is a less known metastable bulk $InPO_4$ structure, beta phase [42] (space group 62). In fact, the beta $InPO_4$ was found by crystallizing amorphous $InPO_4$ [42]. The total energy of the orthorhombic beta $InPO_4$ is close to the ground state value (41 meV per atom larger). The lattice parameter values of $a = 4.89$ Å, $b = 9.04$ Å and $c = 7.03$ Å were obtained. The beta structure looks quite similar to the ground state structure. The main difference is that the PO_4 tetrahedra have one face along the [0 1 0] direction in the beta structure while the tetrahedra have one edge along the [0 1 0] direction in the ground state structure (Fig. 3). Consequently, the O atoms are well above and below the In atom layers along the [0 1 0] direction within the beta phase. In the ground state structure four O neighbors of an In atom are about at the level of the In atoms along the [0 1 0] direction (Fig. 3), which prevents significant lattice relaxation. An initially coherent $InPO_4$ oxide can be formed by straining the (0 1 0)

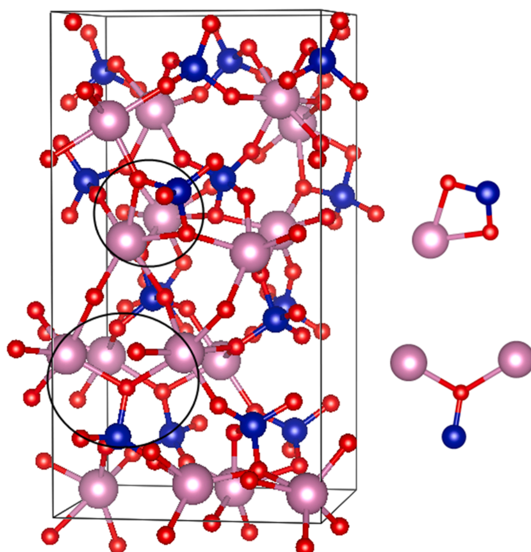

Fig. 6. A slightly disordered $InPO_4$ structure relaxed from the $InPO_4$-b initial structure. The amount of double P-O-In bridges, joining one P atom and one In atom, is considerably decreased as the initial $InPO_4$-a is relaxed. There are no such structural motifs in the initial $InPO_4$-b structure. In the relaxed structure one is found, which is enclosed by a solid curve in the upper part of the unit cell. The amount of P-O-In_2 bridges joining one P atom and two In atoms is increased by relaxation. One of these bridges is shown by a solid curve in the lower part of the unit cell. The top and bottom surfaces of the unit cell have an InP (2 × 2) area. The In, P and O atoms are shown by violet, blue and red spheres, respectively.

face of the beta $InPO_4$ to the InP (1 × 2) (001) area. Although the lattice mismatches are −13.2 % and + 20.8 % along the $InPO_4$ x- and z-directions, the relative total energy of the initially coherent bulk beta $InPO_4$ after relaxation, "gamma" $InPO_4$, is only 59 meV per atom. However, the interface area is increased only 4.7 % by the straining.

The alpha and gamma $InPO_4$ structures are called "quasi-coherent" structures as the structures keep more or less the initial coherent structures on average as the average positions of the different atom types in the oxide films are estimated. The (quasi-)coherence can be broken, *e.g.*, by a dislocation.

The total energies of the quasi-coherent oxides could be compared, *e.g.*, to the tetragonal $InPO_4$, scheelite [34]. The relative total energy of the scheelite is about 98 meV per atom. The stability of the quasi-coherent $InPO_4$ oxides can be compared also to the stability of amorphous Al_2O_3, which was recently reported to be stabilized in thin oxide films on the Al metal [43]. The total energy of the amorphous bulk Al_2O_3 is less stable than the ground state crystalline bulk Al_2O_3 by 0.18 eV per atom [43].

There are two P-O-In bridge bonds from one P atom to the same In atom in the $InPO_4$-a. The number of these double bridges is significantly decreased with structural relaxations. On the other hand, the number of P atoms having two bridges to two In atoms through one O atom (P-O-In_2 bridge) is increased. Initially there are no such structural motifs in the $InPO_4$-b. These local bonding configurations are enclosed by solid curves in Fig. 6. The relaxations are supposed to decrease O-O repulsion and increase In-O and P-O attraction. On the other hand, one can think that the In-O-P interactions replace In-O-In and P-O-P interactions in the $InPO_4$-a. The bond lengths are also optimized locally. The P-O-In_2 bridges cause disorder, because the distance of the In atoms within a P-O-In_2 bridge is smaller than the average In-In distance in the quasi-coherent oxides. There are two orientations of the PO_4 tetrahedra within P atom layers in the gamma quasi-coherent oxide. Consequently, all O atoms within the P-O-In_2 bridges are along the In atom layers in the gamma quasi-coherent $InPO_4$. Therefore, the beta coherent oxide is less disordered than the alpha coherent oxide. It turns out that the In-terminated initially coherent interfaces are more stable than the P-terminated initially coherent interfaces. Neither the In-terminated interface nor the P-terminated interface has vacancies or substitutional atoms.

Relative total energies of the alpha and gamma oxide films are quite close to each other, which suggests that the interface energy of the alpha oxide is smaller than the interface energy of the gamma oxide. The total energy of the alpha oxide film is lower by 37 meV per atom for the thinnest oxide film (one In-O layer and one P-O layer). The gamma oxide is more stable in thicker films (1 – 19 meV per atom). The sum of the interface and surface energy was calculated for the alpha and gamma oxide films using average incremental energy. The values are within −59 - −48 meV/Å^2 and −39 - −27 meV/Å^2 for the alpha and gamma oxides, respectively, with the relative O chemical potential equal to 0 eV. It should be noted that the surface energy is positive. The sum of the interface and surface energies of the incoherent most O-rich P-terminated (100) and In-terminated (001) interface systems are about −62.1 and −0.4 meV/Å^2 with the relative O chemical potential equal to zero. However, it was found in Section 3.1 that the relative total energy of the incoherent In-terminated (001) interface system is lower than that of the incoherent P-terminated (100) interface system, if there is the same number of excess O atoms within both interface systems. The interface energy is strongly dependent on the O content. The quasi-coherent and incoherent In-terminated (001) interface systems have the same number of excess O atoms per interface area. Therefore, the comparison of these interface energies is more relevant. Furthermore, possible inaccuracy of the O chemical potential does not enter into the comparison. It is noted that even smaller interface energy was obtained by forming a quasi-coherent interface using a slice from the structure shown in Fig. 6. The interface energy is about −75 meV/Å^2, because an additional O atom can be inserted into the interface. No systematic search along this direction was performed, but the result shows that it is possible to form more O-rich quasi-coherent interfaces, if the film is thin. The difference between the sums of the interface and surface energies of the (In-terminated) alpha and incoherent (001) interfaces is about 50–60 meV/Å^2. The alpha interface is more stable. It is estimated that the surface energies of the quasi-coherent and incoherent structures are approximately equal, although the exact surface energy of the quasi-coherent structure is not known. Therefore, the interface energy of the quasi-coherent interface is much smaller than the interface energy of the incoherent interface.

The thickest alpha and gamma oxide films and the associated interfaces are shown in Figs. 7 and 8.

The relative total energies of the In-terminated quasi-coherent and incoherent (001) oxide films are estimated for a thickness of two In-O and P-O double layers (about 5.3–6.5 Å; see the beginning of Section 3.1). The total energy of the incoherent system is smaller by only 15 meV per oxide atom. If the incremental energy of the quasi-coherent oxide is used for the μ_{InPO4} in equation (1) corresponding to smaller number of the $InPO_4$ units, the relative energy is about 6 meV per oxide atom. Here the incremental energy of the considered oxide thickness is used. The relative energy of the incoherent oxide film one double layer thick (2.8–3.4 Å) is smaller by about 4 meV per oxide atom. It is remarkable that incoherent and initially coherent thin oxide interface systems have practically the same total energies (but different interface energies). Entropy should favor the somewhat disordered quasi-coherent oxide films over the ordered incoherent films.

Relative total energies of the incoherent In-terminated (001) interface [(001)-In-O] and quasi-coherent alpha and gamma interfaces are shown in Fig. 9. Incremental total energies of quasi-coherent alpha and gamma oxides relative to the bulk total energy of the ground state $InPO_4$ are also shown. Relative total energies and sums of the interface and surface energies for some interface systems are shown in Table 2. Relative total energies of some bulk $InPO_4$ oxides are also shown.

The gap state density of several quasi-coherent interfaces is small or zero. This is difficult to estimate accurately, because possible gap states

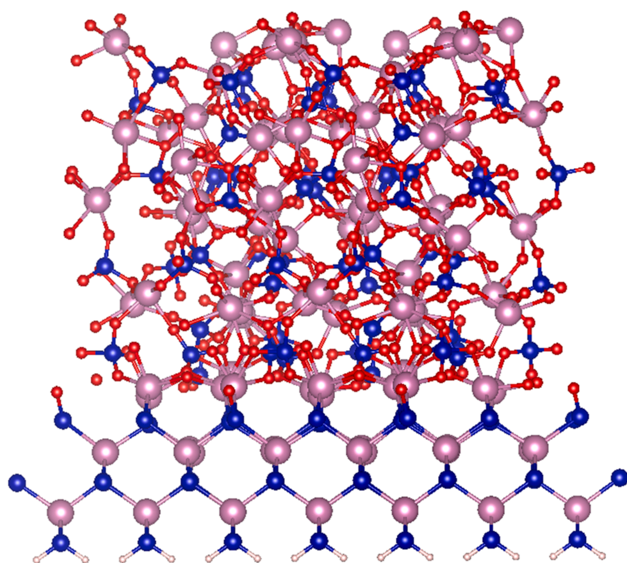

Fig. 7. An interface structure obtained using the unstable initial $InPO_4$-b structure (alpha $InPO_4$ oxide). The thickness of the oxide is about 18 Å. The In, P, O and pseudo-hydrogen atoms are shown by violet, blue, red and grey spheres, respectively.

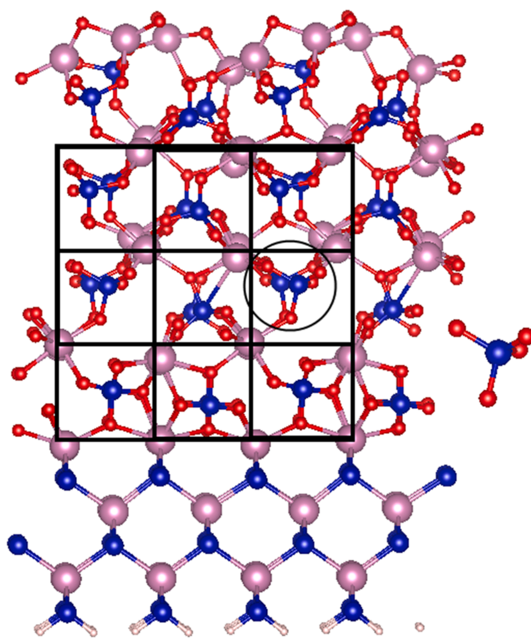

Fig. 8. An interface structure obtained using the initial beta $InPO_4$ structure (gamma $InPO_4$ oxide). The thickness of the oxide is about 17 Å. The interface is quasi-coherent as the atoms occupy more or less the coherent positions on average which is described by a grid. The initial orientation of a PO_4 tetrahedron, one face of a tetrahedron above or below an In atom layer, can be seen enclosed by a solid curve. The In, P, O and pseudo-hydrogen atoms are shown by violet, blue, red and grey spheres, respectively.

are close to the bottom of the conduction band. Fig. 10 shows the density of states curves for a quasi-coherent interface system and for a pure InP slab pseudo-hydrogenated on both surfaces. The thickness of the InP part is five double layers in both systems. The size of the band gap is about 1.0 eV in the pure InP slab, whereas the size of the band gap is about 0.2 eV smaller in the interface system. The absolute value of the band gap is not relevant here, because the GGA underestimates the band gap and in practice the slab construction overestimates the band gap due

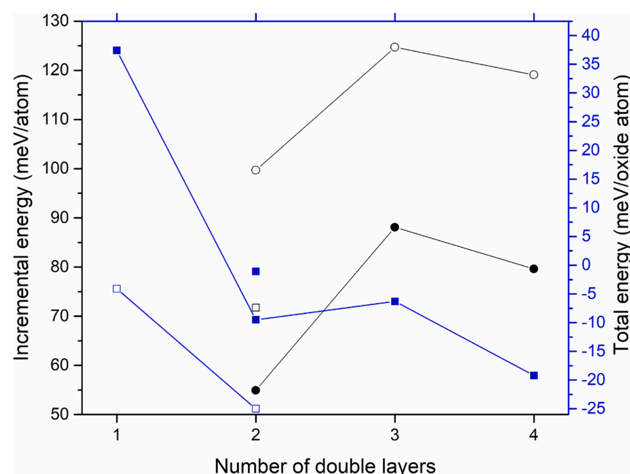

Fig. 9. Incremental total energies (meV/atom) of quasi-coherent alpha (open circles) and gamma (solid circles) $InPO_4$ relative to the total energy of the ground state $InPO_4$. The incremental energies obtained from the thinnest slabs [differences between two and one double layers (DL)] are smaller than the other incremental energies, which is attributed to slightly different surface energies of the thinnest oxide films (one DL). It is concluded that the structure of the quasi-coherent gamma oxide deviates slightly from the corresponding structure obtained from a bulk calculation, which is reflected in incremental total energies (total energy of the gamma oxide obtained from a bulk calculation is about 58.8 meV per atom). The incremental bulk total energy of the ground state $InPO_4$ bulk is only 0.6 meV per atom smaller than the total energy obtained from a bulk calculation. Total energies of the incoherent In-terminated (001) (open squares) and quasi-coherent gamma (solid squares) oxides relative to the quasi-coherent alpha oxide as a function of the film thickness ($InPO_4$ oxide content equal to the quasi-coherent film). The lone squares describe oxide content equal to the incoherent film.

Table 2
Relative total energies (ΔE_{tot}) of ground state and quasi-coherent alpha and gamma bulk $InPO_4$ oxides. These total energies are obtained from bulk calculations. Relative total energies and the sums of the interface and surface energies ($\gamma_I + \gamma_S$) of the incoherent In-terminated (001) interface, incoherent P-terminated (100) interfaces and quasi-coherent alpha and gamma interfaces. The "(100)-P-O-0.2" denotes the interface obtained from the "(100)-P-O" by removing 0.2 excess O atoms per (1 × 1) interface area. The double layers (DL) consist of In-O and P-O layers or In-P-O and O layers [(100) interfaces] (see Section 3.1). Comparison of the total energies between the In-terminated (001) and P-terminated (100) incoherent interfaces corresponds to the situation, in which the number of the excess O atoms is the same in both systems. This is discussed in Section 3.1. The sums of the interface and surface energies are given for two different values of the relative chemical potential of the O atom ($\Delta\mu_O$).

	ΔE_{tot}(meV/oxide atom)	$\gamma_I + \gamma_S$ (meV/Å^2) $\Delta\mu_O = 0.0$ eV	$\gamma_I + \gamma_S$ (meV/Å^2)$\Delta\mu_O = 1.0$ eV
ground state bulk	0.0		
alpha bulk	117.5		
gamma bulk	58.8		
(001)-In-O 1 DL	0.0	−23.2	18.4
alpha 1 DL	4.1	−54.3	−12.7
gamma 1 DL	41.5	−26.8	14.8
(001)-In-O 2 DL	0.0	−0.4	41.2
alpha 2 DL	7.4; 25.0	−59.2	−38.9
gamma 2 DL	6.3; 15.5	−17.6	2.7
(100)-P-O 3 DL	118.1	−62.1	21.2
(100)-P-O-0.2 3 DL	113.1	−25.6	46.6

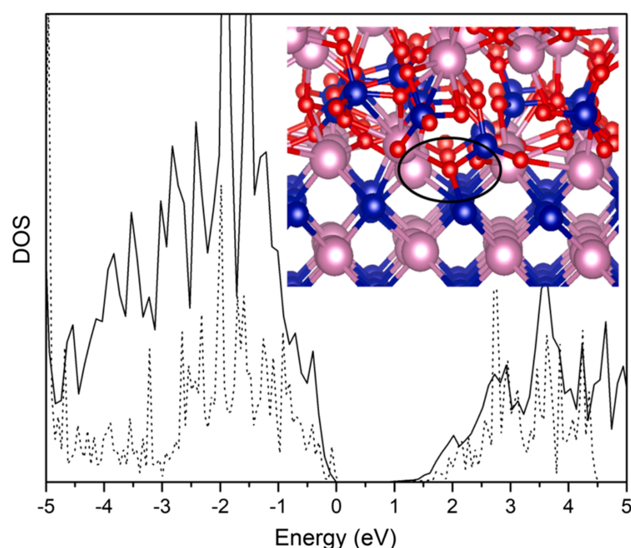

Fig. 10. The density of states (DOS) curve of a quasi-coherent interface system (solid curve) and an InP slab pseudo-hydrogenized on both surfaces (dotted curve). The thickness of the InP part is five double layers in both systems. Zero energy corresponds to the highest occupied state. The gap state density of the interface system is very small or zero. Inset shows a defect type consisting of an O atom inserted into a substrate In-P bond, which causes distinct gap states. The In, P and O atoms are shown by violet, blue and red spheres, respectively.

to limited slab thickness. The difference of 0.2 eV may be due to the fact that the oxide film decreases the overestimation of the band gap caused by the slab construction compared to the pseudo-hydrogenation on both surfaces. In any case the gap state density is very small, if not zero. However, in some quasi-coherent interface systems there are distinct gap states in the mid or lower parts of the band gap. These gap states are caused by O atoms inserted into the substrate In-P bonds shown in the Fig. 10. P-terminated interfaces do not show an energy gap.

The Fermi level pinning at the oxidized GaAs interfaces has been attributed to As dimers and/or As dangling bonds [13,14,44]. Our results point out that the Fermi level pinning might be attributed also to oxidized substrate In-P bonds at least at the InP interfaces. The oxidized In-P substrate bond defects were found in thicker or non-stoichiometric, In-riched, oxide films.

It was found that it is energetically rather favorable to substitute an In atom by a P atom within an initially coherent oxide, whereas it is energetically very unfavorable to substitute a P atom by an In atom. However, it is energetically rather favorable to insert additional In atoms into an initially coherent oxide. (All these modifications have to be balanced by a correct number of additional or removed O atoms due to the ECR.) However, deeper layer oxidations are most probably energetically more favorable. The P substitutions also increase atomic in-plane density, because a P substitution is accompanied by an inserted O atom. In-plane atomic density increase is favored as the (almost) stoichiometric initially coherent oxide film favors in-plane shrinking. Full account of different oxide concentrations is well beyond the present study. However, these results are important as they show that different compositions might be realistically described using the quasi-coherent model. The quasi-coherent, disordered oxide structure is different, *e.g.*, from the disordered SiO_2 structure, because the In-O-P bonds are favored. Thus, the oxide structure tends to be layered.

Different layered structures were proposed based on the experimental photoemission spectra [45,46]. However, the interpretation was challenged and it was proposed that the oxide is a microscopic mixture of different oxide compositions [47]. In any case, composition variations were found in direction perpendicular to the interface. These variations, found at lower growth temperatures, were attributed to slow diffusion of the P [45,48] or evaporation of the P or P_2O_5 [47]. Experimental studies propose P-enrichment at the interface based on a core-level shift similar to elemental P. Our core-level results, calculated using the initial state model (which ignores core–hole relaxation), show that semiconductor P atoms below the interface layer without O neighbors or with one O neighbor show core-level shifts similar to the elemental P. Furthermore, our results suggest that the found In-enrichment at outer part of the oxide film might have also a thermodynamic, and not (purely) kinetic, origin.

Ordered native III-V oxide thin films were experimentally found and these films turned out to have small gap state densities [7,8]. It is probable that these thin oxide films have unstable or metastable structures due to the lattice mismatch and periodicity of the found oxide films. Our results show that these ordered oxide structures, which are unknown, can be stabilized by the interface energy. It might be that (almost) stoichiometric composition close to the interface is needed to grow these oxides, which might partially explain the sensitivity of the growth to oxygen pressure. Our results imply that the Fermi level pinning may be caused by oxidized substrate III-V bonds. These defects become more probable as disorder is increased by the thickness of the somewhat disordered oxide film or non-stoichiometries of the oxide.

Preliminary results concerning band offsets show that (valence) band offsets across the incoherent and quasi-coherent interfaces have similar values. The local potentials at the atom sites are larger, and thus the initial state core-level shifts are smaller, within the gamma oxide than within the alpha oxide and the ground state ("incoherent") oxide, which have rather similar average values. However, probably a dislocation can release strain within the gamma oxide film increasing the core-level shifts. There is a much larger scatter in individual atom site potentials within the quasi-coherent oxides as expected. The average core-level shifts for the alpha oxide and the ground state oxide are about the same or slightly larger than those obtained from bulk calculations [32].

Interfaces for different oxide compounds can also be formed using the initially coherent model. The initially coherent interface presented above ($InPO_4$-a) was used as an initial model for P_2O_5/InP interface. A model with three In-O and P-O double layers was used. An In-O layer and a P-O layer were interchanged to get three successive In-O layers and three successive P-O layers. Some atomic relaxations were performed after which the two topmost In-O layers were removed and two O atoms were introduced within the mid P-O layer to obtain correct stoichiometry. Correct atom coordinations were preserved. The topmost In-O layer is used as a surface layer to stabilize the system, because stable reconstructions for the P_2O_5 surface are not known. An extra O atom (having only one nearest neighbor atom), in addition to a full In-O layer as a top layer, has to be introduced due to the ECR. However, an In-In dimer bond is formed at the interface to which the extra O atom, initially at an energetically quite unfavorable position, can be shifted. Thus, the ECR is satisfied by a stable interface layer including an extra O atom. The formed P_2O_5 oxide is about 0.16 eV per atom less stable than the bulk P_2O_5, which is considered to be a satisfactory result. The DOS reveals no distinct gap states. This result reiterates the finding above according to which partially oxidized substrate P atoms are harmful.

4. Conclusions

It was shown in this work that the InP native oxide (quasi-)coherent interface has a much smaller interface energy than the incoherent interface has. It was also shown that the interface energy can stabilize unstable and metastable oxide structures in thin III-V native oxide films. Relatively small strain energy and configuration match imply a small interface energy. Results suggest that the (quasi-)coherence is an important property, which may govern growth of the III-V oxide interfaces. It is possible that the interface energy causes the disordered structure of the InP native oxides grown at temperatures under 650 °C [45]. The oxide may be grown as somewhat disordered in thin oxide films and the oxide is trapped into the disordered state kinetically in thicker oxide films. These are important results giving new insights into

oxide growth as very little is known of the (native) oxide interface structures of the III-V semiconductors.

Generally In-terminated interfaces show only small or zero gap state density. However, oxidized substrate In-P bonds and partially oxidized P atoms at the interface layer show distinct gap states. These are alternative defect types explaining the Fermi level pinning at least at the InP native oxide interfaces. Experimental results were discussed on the basis of the results found. A core-level shift similar to metallic P found experimentally has been previously explained by elemental P close to the interface. Our initial state core-level shifts show that similar core-level shifts can be attributed to semiconductor P atoms close to the interface with zero or one O atom neighbors. Our results suggest that In-enrichment of the outer layers of the oxide film might also have a thermodynamic origin.

Several complex quasi-coherent and incoherent $InPO_4$/InP interface structures were constructed. General principles to build initially coherent and incoherent model interfaces were clarified. The relatively low interface and total energies show that the quasi-coherent oxide models, including also non-stoichiometric oxides, are reasonable to be used in further studies. The initially coherent or quasi-coherent interface model is relatively simple for computation and interpretation and it does not include substitutional atoms or vacancies. The ECR is satisfied by a designed low energy surface reconstruction.

More complicated or advanced interface models including, *e.g.*, dislocations or non-planar surface structure can be based on the introduced quasi-coherent model. The model can be used to study, *e.g.*, band offsets, core-level shifts, defect states, composition variations, surface morphology and diffusion.

CRediT authorship contribution statement

M.P.J. Punkkinen: Conceptualization, Investigation, Methodology, Visualization, Writing – original draft. **A. Lahti:** Investigation, Methodology, Writing – review & editing. **J. Huhtala:** Visualization, Writing – review & editing. **J.-P. Lehtiö:** Writing – review & editing. **Z.J. Rad:** Writing – review & editing. **M. Kuzmin:** Writing – review & editing. **P. Laukkanen:** Writing – review & editing. **K. Kokko:** Writing – review & editing.

Declaration of Competing Interest

The authors declare that they have no known competing financial interests or personal relationships that could have appeared to influence the work reported in this paper.

Acknowledgments

The Magnus Ehrnrooth Foundation is acknowledged for financial support (A. L.). The computer resources of the Finnish IT Center for Science (CSC) and the FGCI project (Finland) are acknowledged.

References

[1] A.M. Kolpak, S. Ismail-Beigi, Thermodynamic stability and growth kinetics of epitaxial $SrTiO_3$ on silicon, Phys. Rev. B 83 (2011), 165318, https://doi.org/10.1103/PhysRevB.83.165318.
[2] J. Robertson, L. Lin, Bonding principles of passivation mechanism at III-V-oxide interfaces, Appl. Phys. Lett. 99 (22) (2011), 222906, https://doi.org/10.1063/1.3665061.
[3] M.D. Pashley, Electron counting model and its application to island structures on molecular-beam epitaxy grown GaAs(001) and ZnSe(001), Phys. Rev. B 40 (15) (1989) 10481–10487, https://doi.org/10.1103/PhysRevB.40.10481.
[4] J. Robertson, Y. Guo, L. Lin, Defect state passivation at III-V oxide interfaces for complementary metal-oxide-semiconductor devices, J. Appl. Phys. 117 (11) (2015) 112806, https://doi.org/10.1063/1.4913832.
[5] J.A. del Alamo, Nanometre-scale electronics with III-V compound semiconductors, Nature 479 (7373) (2011) 317–323, https://doi.org/10.1038/nature10677.
[6] H. Ko, K. Takei, R. Kapadia, S. Chuang, H. Fang, P.W. Leu, K. Ganapathi, E. Plis, H. S. Kim, S.-Y. Chen, M. Madsen, A.C. Ford, Y.-L. Chueh, S. Krishna, S. Salahuddin, A. Javey, Ultrathin compound semiconductor on insulator layers for high-performance nanoscale transistors, Nature 468 (7321) (2010) 286–289, https://doi.org/10.1038/nature09541.
[7] M.P.J. Punkkinen, P. Laukkanen, J. Lång, M. Kuzmin, M. Tuominen, V. Tuominen, J. Dahl, M. Pessa, M. Guina, K. Kokko, J. Sadowski, B. Johansson, I.J. Väyrynen, L. Vitos, Oxidized In-containing III-V(100) surfaces: Formation of crystalline oxide films and semiconductor-oxide interfaces, Phys. Rev. B 83 (2011), 245401, https://doi.org/10.1103/PhysRevB.83.195329.
[8] C.H. Wang, S.W. Wang, G. Doornbos, G. Astromskas, K. Bhuwalka, R. Contreras-Guerrero, M. Edirisooriya, J.S. Rojas-Ramirez, G. Vellianitis, R. Oxland, M. C. Holland, C.H. Hsieh, P. Ramvall, E. Lind, W.C. Hsu, L.-E. Wernersson, R. Droopad, M. Passlack, C.H. Diaz, InAs hole inversion and bandgap interface state density of 2×10^{11} cm^{-2} eV^{-1} at HfO_2/InAs interfaces, Appl. Phys. Lett. 103 (2013), 143510, https://doi.org/10.1063/1.4820477.
[9] L.E. Black, A. Cavalli, M.A. Verheijen, J.E.M. Haverkort, E.P.A.M. Bakkers, W.M. M. Kessels, Effective surface passivation of InP Nanowires by atomic-layer-deposited Al_2O_3 with PO_x interlayer, Nano Lett. 17 (10) (2017) 6287–6294, https://doi.org/10.1021/acs.nanolett.7b0297210.1021/acs.nanolett.7b02972.s001.
[10] C.W. Wilmsen (Ed.), Physics and Chemistry of III-V Compound Semiconductor Interfaces, Springer US, Boston, MA, 1985.
[11] M. Scarrozza, G. Pourtois, M. Houssa, M. Caymax, A. Stesmans, M. Meuris, M. M. Heyns, A first-principles study of the structural and electronic properties of III-V/thermal oxide interfaces, Microelectron Eng. 86 (7-9) (2009) 1747–1750, https://doi.org/10.1016/j.mee.2009.03.110.
[12] W. Wang, K.a. Xiong, G. Lee, M. Huang, R.M. Wallace, K. Cho, Origin of HfO_2/GaAs interface states and interface passivation: A first principles study, Appl. Surf. Sci. 256 (22) (2010) 6569–6573.
[13] J. Robertson, L. Lin, Defect gap states on III-V semiconductor-oxide interfaces, Microelectron. Eng. 88 (2011) 1440–1443, https://doi.org/10.1016/j.mee.2011.03.134.
[14] L. Lin, J. Robertson, Defect states at III-V semiconductor oxide interfaces, Appl. Phys. Lett. 98 (8) (2011) 082903, https://doi.org/10.1063/1.3556619.
[15] Weichao Wang, Ka Xiong, Robert M. Wallace, Kyeongjae Cho, Impact of Interfacial Oxygen Content on Bonding, Stability, Band Offsets, and Interface States of GaAs: HfO_2 Interfaces, J. Phys. Chem. C 114 (51) (2010) 22610–22618, https://doi.org/10.1021/jp107880r.
[16] K. C. Santosh, Hong Dong, Roberto C. Longo, Weichao Wang, Ka Xiong, Robert M. Wallace, Kyeongjae Cho, Electronic properties of InP/HfO2 (001) interface: Band offsets and oxygen dependence, J. Appl. Phys. 115 (2014) 023703. https://doi.org/10.1063/1.4861177.
[17] A. Lahti, H. Levämäki, J. Mäkelä, M. Tuominen, M. Yasir, J. Dahl, M. Kuzmin, P. Laukkanen, K. Kokko, M.P.J. Punkkinen, Electronic structure and relative stability of the coherent and semi-coherent HfO_2/III-V interfaces, Appl. Surf. Sci. 427 (2018) 243–252, https://doi.org/10.1016/j.apsusc.2017.08.185.
[18] Giacomo Miceli, Alfredo Pasquarello, Accurate determination of charge transition levels of the As-As dimer defect at GaAs/oxide interfaces through hybrid functionals, Appl. Phys. Lett. 103 (4) (2013) 041602, https://doi.org/10.1063/1.4816661.
[19] Giacomo Miceli, Alfredo Pasquarello, First principles study of As 2*p* core-level shifts at GaAs/Al_2O_3 interfaces, Appl. Phys. Lett. 102 (20) (2013) 201607, https://doi.org/10.1063/1.4807730.
[20] Eun Ji Kim, Evgueni Chagarov, Joël Cagnon, Yu Yuan, Andrew C. Kummel, Peter M. Asbeck, Susanne Stemmer, Krishna C. Saraswat, Paul C. McIntyre, Atomically abrupt and unpinned Al2O3/In0.53Ga0.47As interfaces: Experiment and simulation, J. Appl. Phys. 106 (2009) 124508. https://doi.org/10.1063/1.3266006.
[21] M. Scarrozza, G. Pourtois, M. Houssa, M. Caymax, M. Meuris, M.M. Heyns, A. Stesmans, Adsorption of molecular oxygen on the reconstructed β2(2×4)-GaAs (001) surface: A first-principles study, Surf. Sci. 603 (1) (2009) 203–208, https://doi.org/10.1016/j.susc.2008.11.002.
[22] Jian Shen, Evgueni A. Chagarov, Daarby L. Feldwinn, Wilhelm Melitz, Nancy M. Santagata, Andrew C. Kummel, Ravi Droopad, Matthias Passlack, Scanning tunneling microscopy/spectroscopy study of atomic and electronic structures of In2O on InAs and In0.53Ga0.47As(001)-(4×2) surfaces, J. Chem. Phys. 133 (2010) 164704. https://doi.org/10.1063/1.3497040.
[23] Isaac Azahel Ruiz Alvarado, Marsel Karmo, Erich Runge, Wolf Gero Schmidt, InP and AlInP(001)(2×4) Surface Oxidation from Density Functional Theory, ACS Omega 6 (9) (2021) 6297–6304, https://doi.org/10.1021/acsomega.0c0601910.1021/acsomega.0c06019.s001.
[24] John P. Perdew, Kieron Burke, Matthias Ernzerhof, Generalized Gradient Approximation Made Simple, Phys. Rev. Lett. 77 (18) (1996) 3865–3868, https://doi.org/10.1103/PhysRevLett.77.3865.
[25] P.E. Blöchl, Projector augmented-wave method, Phys. Rev. B 50 (24) (1994) 17953–17979, https://doi.org/10.1103/PhysRevB.50.17953.
[26] G. Kresse, D. Joubert, From ultrasoft pseudopotentials to the projector augmented-wave method, Phys. Rev. B 59 (3) (1999) 1758–1775, https://doi.org/10.1103/PhysRevB.59.1758.
[27] G. Kresse, J. Hafner, *Ab initio* molecular dynamics for liquid metals, Phys. Rev. B 47 (1) (1993) 558–561, https://doi.org/10.1103/PhysRevB.47.558.
[28] G. Kresse, J. Hafner, *Ab initio* molecular-dynamics simulation of the liquid-metal-amorphous-semiconductor transition in germanium, Phys. Rev. B 49 (20) (1994) 14251–14269, https://doi.org/10.1103/PhysRevB.49.14251.
[29] G. Kresse, J. Furthmüller, Efficiency of ab-initio total energy calculations for metals and semiconductors using a plane-wave basis set, Comput. Mat. Sci. 6 (1) (1996) 15–50, https://doi.org/10.1016/0927-0256(96)00008-0.

[30] G. Kresse, J. Furthmüller, Efficient iterative schemes for *ab initio* total-energy calculations using a plane-wave basis set, Phys. Rev. B 54 (16) (1996) 11169–11186, https://doi.org/10.1103/PhysRevB.54.11169.
[31] Hendrik J. Monkhorst, James D. Pack, Special points for Brillouin-zone integrations, Phys. Rev. B 13 (12) (1976) 5188–5192, https://doi.org/10.1103/PhysRevB.13.5188.
[32] J. Mäkelä, A. Lahti, M. Tuominen, M. Yasir, M. Kuzmin, P. Laukkanen, K. Kokko, M.P.J. Punkkinen, H. Dong, B. Brennan, R.M. Wallace, Unusual oxidation-induced core-level shifts at the HfO2/InP interface, Sci. Rep. 9 (2019) 1462, https://doi.org/10.1038/s41598-018-37518-2.
[33] A. Debernardi, C. Wiemer, M. Fanciulli, Epitaxial phase of hafnium dioxide for ultrascaled electronics, Phys. Rev. B 76 (2007), 155405, https://doi.org/10.1103/PhysRevB.76.155405.
[34] S. López-Moreno, D. Errandonea, *Ab initio* prediction of pressure-induced structural phase transitions of $CrVO_4$-type orthophosphates, Phys. Rev. B 86 (2012), 104112, https://doi.org/10.1103/PhysRevB.86.104112.
[35] E. Kaxiras, Y. Bar-Yam, J.D. Joannopoulos, K.C. Pandey, *Ab initio* theory of polar semiconductor surfaces. I. Methodology and the (2×2) reconstructions of GaAs (111), Phys. Rev. B 35 (18) (1987) 9625–9635, https://doi.org/10.1103/PhysRevB.35.9625.
[36] G.-X. Qian, R.M. Martin, D.J. Chadi, First-principles study of the atomic reconstructions and energies of Ga- and As-stabilized GaAs(100) surfaces, Phys. Rev. B 38 (1988) 7649, https://doi.org/10.1103/PhysRevB.38.7649.
[37] J.C. Boettger, Nonconvergence of surface energies obtained from thin-film calculations, Phys. Rev. B 49 (23) (1994) 16798–16800, https://doi.org/10.1103/PhysRevB.49.16798.
[38] N. Ridley, Densities of some indium solid solutions, J. Less-Common Metals 8 (5) (1965) 354–357, https://doi.org/10.1016/0022-5088(65)90071-8.
[39] A. Brown, S. Rundqvist, Refinement of the crystal structure of black phosphorus, Acta Cryst. 19 (4) (1965) 684–685, https://doi.org/10.1107/S0365110X65004140.
[40] S.Zn. Karazhanov, P. Ravindran, P. Vajeeston, A. Ulyashin, T.G. Finstad, H. Fjällvåg, Phase stability, electronic structure, and optical properties of indium oxide polytypes, Phys. Rev. B 76 (2007), 075129, https://doi.org/10.1103/PhysRevB.76.075129.
[41] El Hassan Arbib, Brahim Elouadi, Jean Pierre Chamanide, Jacques Darriet, New Refinement of the Crystal Structure of o-P2O5, J. Sol. State Chem. 127 (1996) 350–353, https://doi.org/10.1006/jssc.1996.0393.
[42] V. Peltier, P. Deniard, R. Brec, R. Marchand, Synthese et structure d'une nouvelle variete de phosphate d'indium : $InPO_4$-β, C. R. Acad. Sci. Paris 1 (1998) 57–62, https://doi.org/10.1016/S1251-8069(97)86261-6.
[43] M. Aykol, Kristin A. Persson, Oxidation Protection with Amorphous Surface Oxides: Thermodynamic Insights from Ab Initio Simulations on Aluminum, ACS Appl. Mater. Interfaces 10 (3) (2018) 3039–3045, https://doi.org/10.1021/acsami.7b14868.
[44] Davide Colleoni, Giacomo Miceli, Alfredo Pasquarello, Origin of Fermi-level pinning at GaAs surfaces and interfaces, J. Phys.: Condens. Matter 26 (49) (2014) 492202, https://doi.org/10.1088/0953-8984/26/49/492202.
[45] A. Nelson, K. Geib, C.W. Wilmsen, Composition and structure of thermal oxides of indium phosphide, J. Appl. Phys. 54 (1983) 4134–4140, https://doi.org/10.1063/1.332547.
[46] M. Losurdo, P. Capezzuto, G. Bruno, Study of the H_2 remote plasma cleaning of InP substrate for epitaxial growth, J. Vac. Sci. Technol. B 14 (1996) 691–697, https://doi.org/10.1116/1.589158.
[47] E. Berignat, G. Hollinger, Y. Robach, A study of thermal oxide-InP interfaces, Surf. Sci. 189–190 (1987) 353–361, https://doi.org/10.1016/S0039-6028(87)80453-3.
[48] E.A. Irene, A comparison of the oxidation and passivation of Si, Ge and InP, Mater. Sci. Forum 185–188 (1995) 37–42, https://doi.org/10.4028/www.scientific.net/MSF.185-188.37.